

FATIGUE ANALYSIS OF JACKET SUPPORT STRUCTURE FOR OFFSHORE WIND TURBINES

Nguyen Van Vuong^{a,*}, Mai Hong Quan^a

^a*Faculty of Coastal and Offshore Engineering, National University of Civil Engineering, 55 Giai Phong road, Hai Ba Trung district, Hanoi, Vietnam*

Article history:

Received 01 October 2018, Revised 19 November 2018, Accepted 31 January 2019

Abstract

In the past few decades and up to now, the fossil energy has exerted tremendous impacts on human environments and gives rise to greenhouse effects while the wind power, especially in offshore region, is an attractive renewable energy resource. For offshore fixed wind turbine, stronger foundation like jacket structure has a good applicability for deeper water depth. Once water depth increases, dynamic responses of offshore wind turbine (OWT) support structures become an important issue. The primary factor will be the total height of support structure increases when wind turbine is installed at offshore locations with deeper water depth, in other words the fatigue life of each components of support structure decrease. The other one will experience more wind forces due to its large blades, apart from wave, current forces, when makes a comparison with offshore oil and gas platforms. Summing up two above reasons, fatigue analysis, in this research, is a crucial aspect for design of offshore wind turbine structures which are subjected to time series wind, wave loads and carried out by aiding of SACS software for model simulation (P-M rules and S-N curves) and Matlab code. Results show that the fatigue life of OWT is decreased accordingly by increasing the wind speed acting on the blades, especially with the simultaneous interaction between wind and wind-induced wave. Hence, this should be considered in wind turbine design.

Keywords: offshore wind turbine; Jacket structure; fatigue analysis; P-M rules; S-N curves.

[https://doi.org/10.31814/stce.nuce2019-13\(1\)-05](https://doi.org/10.31814/stce.nuce2019-13(1)-05) © 2019 National University of Civil Engineering

1. Introduction

Wind energy has been utilized for mankind in terms of electricity production for thousands of years [1]. Wind energy onshore nowadays is a mature industry responsible for meeting a part of the energy needs in countries around the globe. In the recent few decades, offshore fixed wind turbines have been all installed in shallow water depth off the coast of Europe (< 30 m) [2], with the typical gravity-based supports of Mono-pile and Tripod structures. However, there is strong demand that the application of offshore fixed wind turbine could be extended to deep water where winds are stronger and steadier than on land [3]. Once water depth increases, dynamic responses of offshore wind turbine support structures become an important issue. Although there is a potential for more wind turbines to be erected in offshore locations in order to achieve a greater wind energy harvest, the access to turbines for maintenance will be restricted. Besides, the fatigue analysis of offshore oil and gas platforms have been studied in a comprehensive way for ages, but for wind turbine in general and offshore wind turbine in particular, this issue is still a new field and a restriction to scientists. Thus, the objective of

*Corresponding author. *E-mail address:* vuongnv@nuce.edu.vn (Vuong, N. V.)

the article is to analyze fatigue life of components of wind turbine support structure and eventually predict the expected lifetime of OWT.

The paper is carried out by applying the fatigue knowledge for the offshore wind turbine, any computing details are conducted by MATLAB code program and SACS software. Applications of the method to offshore wind turbine with Jacket support structure are illustrated in the following sections and ending up with conclusions and highlights for future research.

2. Load effects analysis of offshore wind turbine

2.1. Wind load

a. Wind profiles and turbulence

The wind velocity measured in the field shows variations in space, time and direction and is composed by two parts: a mean (or slowly variable) and a stochastic part (turbulence) as showing in Fig. 1. The total wind velocity in any points of structure is the sum of the average wind velocity and turbulent wind velocity [4]:

$$\{V(z, t)\} = \{\bar{v}(z)\} + \{v(t)\} \tag{1}$$

where $\bar{v}(z)$ is average wind velocity; $v(t)$ is turbulent wind velocity.

The geometric parameters in Fig. 2 conclude: the water mean depth (h), the hub height above the mean water level (H) and the blades length (or rotor radius) (R). Accepting approximately the dynamic component of the wind according to the Weibull distribution law. Weibull probability distribution (the so-called probability distribution Rosin-Rammler) is a common form used to describe the occurrence of extreme quantities in meteorology, hydrology and weather forecasts such as floods, waves and winds. In this paper, the Weibull probability distribution is used to calculate the cumulative frequencies of wind velocity in any directions.

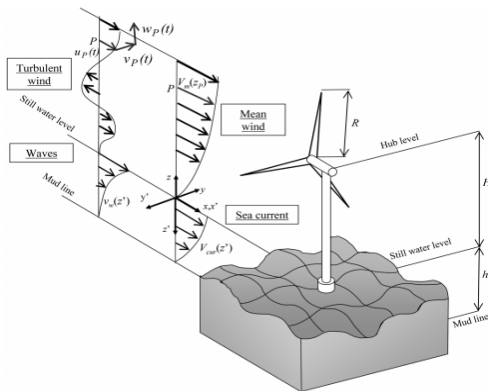


Figure 1. Wind, wave and current actions configuration [5]

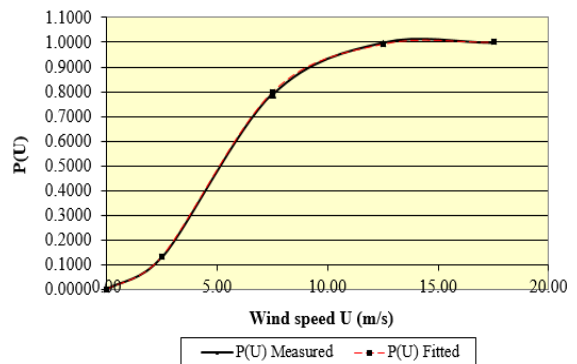


Figure 2. Distribution curve of wind speed

b. Cumulative frequency distribution function of wind velocity according to Weibull

$$P(u) = 1 - \exp \left[- \left(\frac{U}{U_0} \right)^k \right] \tag{2}$$

where U is wind velocity; k is the shape parameter; U_0 is the rate parameter. The distribution curve of Weibull function with different wind speed as shown in Fig. 2.

c. Correlation between significant wave height, period and wind speed

Wind blowing time $t_{x,u}$ is in accordance to wind fetch X , and wind velocity u [6], the time to a state of fully developed sea:

$$t_{x,u} = 77.23 \frac{X^{0.67}}{u^{0.34} g^{0.33}} \quad (3)$$

Significant wave height in accordance with wind velocity u :

$$H_z = H_0 \frac{u_*^2}{g} \quad (4)$$

where

$$H_0 = \lambda_1 x^{m_1}; \quad x = \frac{gX}{u_*^2} \quad (5)$$

$$\lambda_1 = 0.0413; \quad m_1 = \frac{1}{2}; \quad u_* = \sqrt{C_d} u_{10}$$

Zero-crossing average period T_z in accordance with wind velocity u :

$$T_z = T_0 \frac{u_*}{g} \quad (6)$$

where

$$T_0 = \lambda_2 x^{m_2} \quad (7)$$

$$\lambda_1 = 0.751; \quad m_2 = \frac{1}{3}$$

2.2. Wind-induced wave load

a. Sea-state model

Waves are generated by wind blowing over the surface of the sea and are the major source of loading for most offshore structures. At any fixed position in the open sea, the level of the water surface varies randomly due to the passing waves and may be modeled as a steadily stochastic process, standard distribution, Ergodic nature [8]. The wave height H of single wave is normally defined as the total range of $\eta(t)$ in the time interval T_0 between two consecutive zero up-crossing by $\eta(t)$, see Fig. 3.

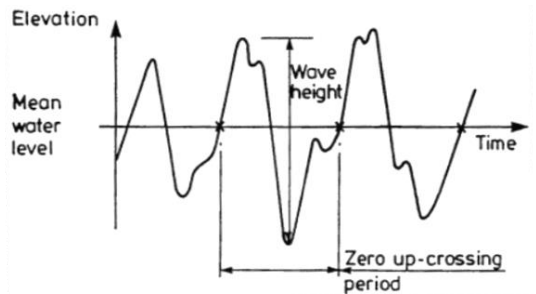


Figure 3. Description of single wave [7]

Recent research has led to a number of semi-empirical expressions for the form of the spectra $S_{\eta\eta}(\omega)$ of water surface elevation $\eta(t)$, (generally called wave spectra). Two commonly used spectra are the Pierson-Moskowitz (P-M) [9] and the JONSWAP [10].

b. Pierson-Moskowitz Spectra (P-M Spectra)

$$S_{\eta\eta}(f) = \frac{Ag^2}{f^5} \exp\left(-B\left(\frac{g}{fU}\right)^4\right) \quad (8)$$

$$A = 4\pi \left(\frac{H_s}{gT_z^2} \right)^2; \quad B = 16\pi^3 \left(\frac{U}{gT_z} \right)^4 \quad (9)$$

where U is wind speed at the height of 19.5 m above sea level; A, B are constants, and P-M spectra with wind speed $U_{19.5} = 15$ m/s is shown in Fig. 4.

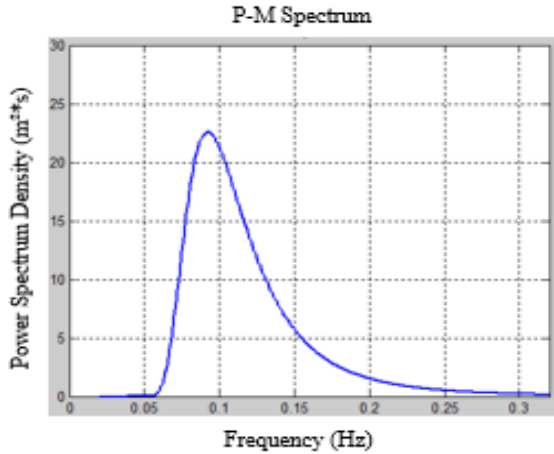


Figure 4. Pierson-Moskowitz and JONSWAP spectrum

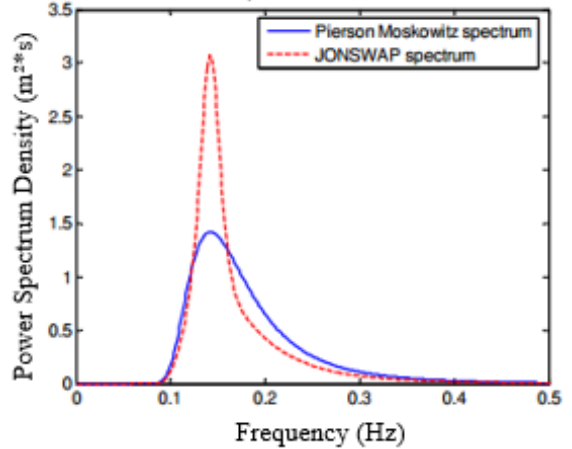


Figure 5. P-M spectrum, wind speed $u_{19.5} = 15$ m/s

c. JONSWAP Spectra

$$S_{\eta\eta}(f) = \frac{ag^2}{(2\pi)^4 f^5} \exp\left(-\frac{5}{4}\left(\frac{\omega}{\omega_m}\right)^{-4}\right) \gamma \exp\left(-\frac{(\omega - \omega_m)^2}{2\sigma^2\omega_m}\right) \quad (10)$$

$$a = 0.046 \left(\frac{X^{-0.22}}{U_{10}^2} \right); \quad \omega_m = \frac{16.04}{(XU_{10})^{0.38}} \quad (11)$$

where X is fetch; U_{10} is wind speed at the height of 10 m above sea level; $\gamma = 0.3; \sigma = 0.08$.

For the purpose of primarily analyzing fatigue of offshore structures, P-M spectra is an appropriate model in the study that deals with the state of sea with maximum wind speed (generating waves under the infinite wind fetch). The most glaring difference between JONSWAP and P-M spectrum with the same wind speed can be seen in Fig. 5.

3. Stochastic dynamics of wind turbine in frequency domain

3.1. The fundamental equation of the stochastic dynamic problem

Differential equation that describes stochastic oscillation of the offshore fix-structure system is as following:

$$M\ddot{U} + C\dot{U} + KU = F(t) \quad (12)$$

where $R_{FF}(\tau)$ is correlation function (self-correlation) of the steadily stochastic process (SSP) $F(t)$, performs Fourier integral transformation (complex form) to $R_{FF}(\tau)$:

$$R_{FF}(\tau) = \int_{-\infty}^{\infty} S_{FF}(\omega) e^{i\omega\tau} d\omega \tag{13}$$

where $S_{FF}(\omega)$ - Spectral density function of SSP $F(t)$, is the Fourier map of the correlation function $R_{FF}(\tau)$:

$$S_{FF}(\omega) = \mathcal{F}R_{FF}(\tau) = \frac{1}{2\pi} \int_{-\infty}^{\infty} R_{FF}(\tau) e^{i\omega\tau} d\tau \tag{14}$$

Formula pairs Eqs. (13) and (14) is called formula Khinchin – Weiner (only applicable to SSP), which play a pivotal role in the method of solving stochastic dynamical problems. Linking to Eq. (14), allows to transform problem to be considered for time-varied correlation function t , to one for frequency-varied density spectral function ω . Fig. 6 describes typical forms of this transform.

3.2. System response in frequency domain

Also applying Khinchin – Wiener formula pairs for stochastic process $u(t)$ [11], [noticing that the input $F(t)$ is SSP, also for output $U(t)$ is SSP], we have:

$$R_{uu}(\tau) = \int_{-\infty}^{\infty} S_{uu}(\omega) e^{i\omega\tau} d\omega \tag{15}$$

$$S_{uu}(\omega) = \frac{1}{2\pi} \int_{-\infty}^{\infty} R_{uu}(\tau) e^{-i\omega\tau} d\tau \tag{16}$$

Applying correlation theory (or spectral theory) – with any theories of SSP into the Eq. (16), obtaining important results:

$$S_{uu}(\omega) = |H(i\omega)|^2 S_{FF}(\omega) \tag{17}$$

In other words: The output spectral density (system response) is equal to the input one (load) multiplied by the square of the transfer function module (Fig. 8).

From Eq. (17) determine the average square (so-called variance) of the response:

$$\sigma_u^2 = \int_0^{\infty} S_{uu}(\omega) d\omega = \int_0^{\infty} |H(i\omega)|^2 S_{FF}(\omega) d\omega \tag{18}$$

where $H(i\omega)$ - transfer function (complex form) also known as “frequency characteristics” of the system, receiving this equation:

$$H(i\omega) = \frac{1}{(K - M\omega^2) + iC\omega} \tag{19}$$

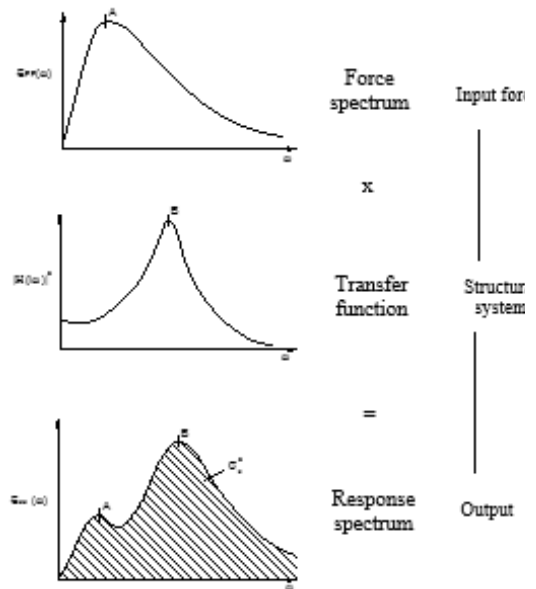


Figure 6. Description of spectral method

4. Fatigue analysis

4.1. Fourier transformation

A spectrum can be used to recreate a time signal. By assuming that the phase angle is distributed randomly, harmonic waves can be recreated based on the power spectrum density at each separate frequency, combined with a randomly picked phase angle. The time series created in this way is never the exact copy of the time series but the spectral parameters are the same, provided that the signal is long enough. Fig. 7 shows the inverse conversion from frequency to time domain as well as the normal transformation from time to frequency domain. For both transformations standard algorithms are available, the most commonly used is the Fast Fourier Transform (FFT) and its Inverse one (IFFT) [12].

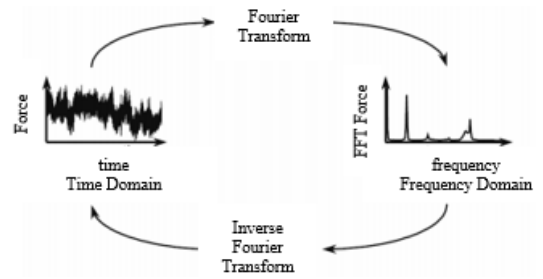


Figure 7. Transformation from time series to frequency domain and vice versa

A time signal can be also used to recreate a spectrum, the power spectrum density per frequency defined as:

$$\frac{1}{2} (S_n^2 / \Delta f) = \frac{1}{2} \{ (A_q^2 + B_q^2) T \} \quad (20)$$

as a function of frequency, where the Fourier coefficients A_q and B_q defined by:

$$A_q = \frac{2}{T} \int_0^T z(t) \cos(2\pi f_q t) dt \quad \text{and} \quad B_q = \frac{2}{T} \int_0^T z(t) \sin(2\pi f_q t) dt \quad (21)$$

When the power spectral density is plotted as a function of frequency, we will obtain a power density spectrum.

4.2. Fatigue analysis in time series

Fatigue is the process of gradual damage done to materials (mainly is steel material) when these are subjected to continually changing stresses. Due to these stress changes, the material slowly deteriorates, initiating cracks which will eventually lead to breaking of the material. Offshore wind turbines are by default subjected to loads varying in time from wind as well as waves. This means that the stress response will also vary continuously, making offshore wind turbine's response to fatigue.

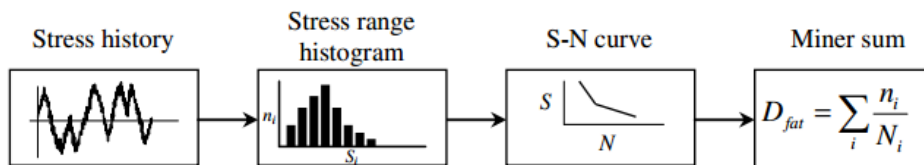


Figure 8. Flowchart of fatigue calculation [13]

The fatigue calculation method for variable stress ranges in the time domain can be summarized by the flowchart in Fig. 8. Calculation of the stresses experienced by the detail being considered under all possible load cases during the lifetime will result in a large number of stress time series. By

filtering the number of stress variations for every stress range class, the Miner sum can be calculated to check whether $D_{fat} < 1.0$.

Fatigue curve linked between the number of stresses S and the number of stress cycles N is revealed as following:

$$N = KS^{-m}, \quad S > 0 \tag{22}$$

where K and m are random variables due to inherent physical and statistical uncertainty. The value of K can depend on the mean stress S_a in the stress cycles. Where K_0 is the value of K from tests with zero mean stress and where S_u is the ultimate tensile strength.

On the above diagram, the index i is the number of stress i^{th} of structure, the ratio of fatigue damage D_{fat} is calculated as the sum of the fatigue damage due to the number of stresses caused in a short sea state.

The magnitude and number of stresses are calculated from fatigue stress data by counting method. To take all peaks into account without doubling, the rain-flow method resembles rain flowing off a pagoda roof as shown in Fig. 9. When the stress time series is rotated 90 degrees, the counting algorithm starts.

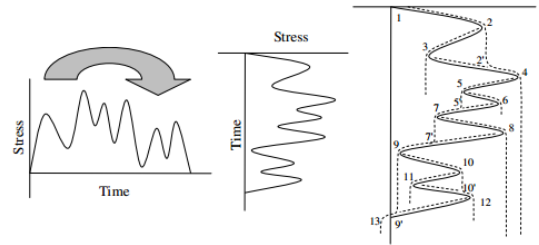


Figure 9. Description of rainflow method [14]

When the method has been performed, the signal is taken apart in a number of half stress range variations, that is, the rain-flow cycle runs only in one direction each time. The mean value of cumulative fatigue damage during 1 year and the maximum mean fatigue lifetime T_{max} of the hot spot are obtained as follows:

$$D_{1year} = \frac{365 \times 24 \times 3600}{T_0} \sum_i \frac{n_i}{N_i}; \quad T_{max} = \frac{[D]}{D_{1year}} \tag{23}$$

where i is investigated stress domain; n_i is the number of stress cycles at the i^{th} load; N_i is the number of cycles until the crashes occur at the i^{th} load; T_0 is the duration of stress in time series; $[D]$ is permissible fatigue, given in used design standard (for offshore structure $[D] = 0.5$, from API standard).

5. Results and discussions

In this paper, the Offshore Jacket Wind Turbine (OJWT) in water depth of 70 m is modeled for analysis showed in Fig. 10. As shown in Fig. 10, a full-scale offshore wind turbine model includes turbine support, transitions, blades and Jacket support. At the top of the support is a 5 MW turbine, the main specifications are listed in Table 1.

a. Structural dimensions

The size of the wind turbine support structure is selected as Fig. 11 for the analysis of fatigue damages under the action of sea environment loads such as waves and wind.

The main dimensions of the entire Jacket support structure with the tower and the wind directions to OJWT are shown in Figs. 12 and 13, respectively. From top to bottom, the Jacket size is 32 m² on the seafloor.

Table 1. Characteristics of offshore wind turbines

Power	5	MW
Cut-out wind speed	25	m/s
Cut-in wind speed	3	m/s
Blade number	3	-
Null diameter	3	m
Blade diameter	126	m
Concentrated mass at top-turbine	120000	kg



Figure 10. 3D model of Jacket support-structure wind turbine

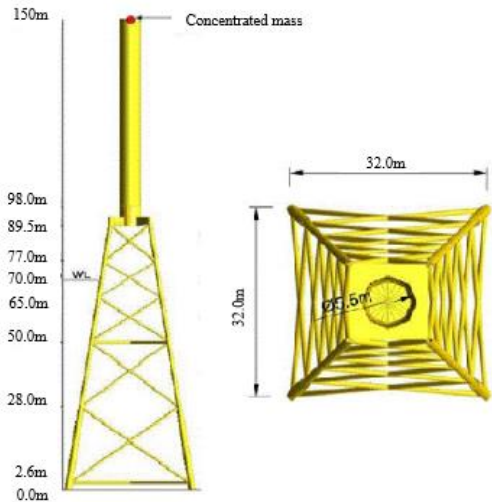


Figure 11. Main dimensions of OJWT

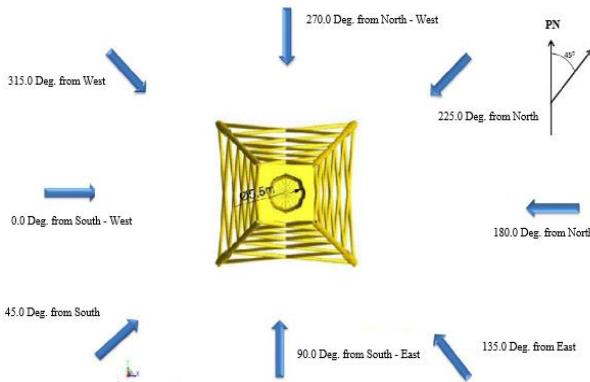


Figure 12. Wave directions to OJWT

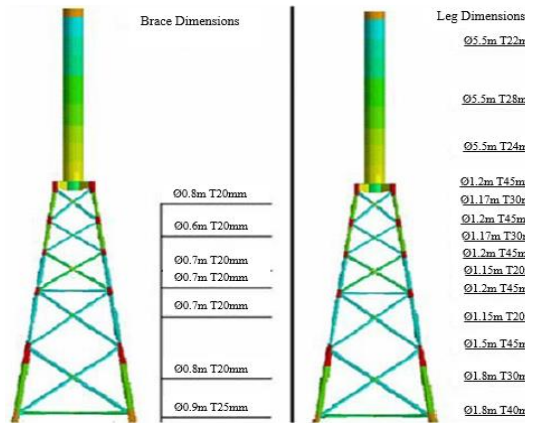


Figure 13. Tower, Brace and diagonal diameters

With regard to the input data of waves and winds, the probability of occurrence of both in the scope of this research is taken in 08 directions as shown in Tables 2 and 3. Each direction is 45 degrees apart before acting on the OJWT. Meanwhile, the prevailing wind directions are the South

West, East and North East and the wind speeds vary from 0 m/s to 20 m/s.

b. Wave parameters

Table 2. Probability of occurrence of wave directions to OJWT

Wave directions	0°	45°	90°	135°	180°	225°	270°	315°	Total
	SW	S	SE	E	NE	N	NW	SW	
Probability (P)	0.3012	0.0353	0.046	0.2629	0.2964	0.0039	0.002	0.0524	1.000

(SW – South West; S – South; SE – South East; E – East; NE – North East; N – North; NW – North West; SW – South West).

c. Wind parameters

Table 3. Probability of occurrence of wind directions to OJWT

Wind Speed (m/s)	Middle Value	Directions								Total
		45	90	135	180	225	270	315	360	
0 - 5	2.50	0.0146	0.0329	0.0337	0.0375	0.0321	0.0148	0.0054	0.0065	0.1774
5 - 10	7.50	0.1653	0.0938	0.0162	0.0299	0.1603	0.0751	0.0056	0.0116	0.5579
10 - 15	12.50	0.1531	0.0036	0.0000	0.0002	0.0515	0.0361	0.0004	0.0084	0.2533
15 - 20	17.50	0.0098	0.0000	0.0000	0.0000	0.0000	0.0000	0.0000	0.0016	0.0115
Total		0.3428	0.1303	0.0498	0.0676	0.2439	0.1260	0.0114	0.0282	1.0000

After taking the estimation of Weibull Parameters for long term distribution of wind speeds in each direction, the fitted parameters U_0 and K are obtained as illustrating in Table 4. The wind data measured in the field is fitted rather precisely with the Weibull distribution function as shown in Fig. 14.

Table 4. The fitted Weibull parameters for wind distribution

Fitted Weibull Parameter	Wind Directions							
	0	45	90	135	180	225	270	315
U_0	6.050	2.750	2.350	4.250	8.250	6.975	3.350	6.725
K	2.200	2.250	2.150	2.250	2.875	1.475	1.500	2.225

d. Results

After obtaining the results of wind turbine analysis from SACS software under hot-spot stress spectrum as showing in Figs. 15 and 16, then utilizes the Fourier transform to convert the hot-spot stress into a time domain for two cases caused by waves and winds as showing in Figs. 17 and 18. In the case of wind turbine systems subjected to both waves and winds is going to take a linear combination of two results due to wave and wind in time series, and obtain the combining results as Fig. 19 shown.

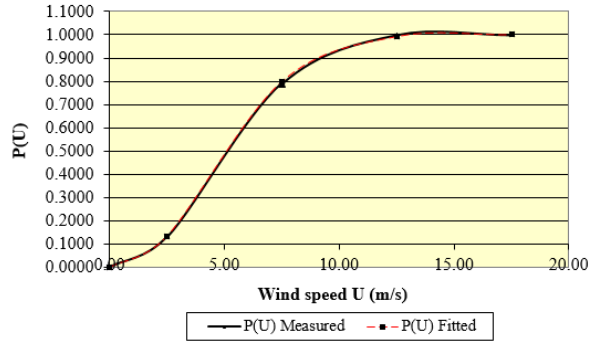


Figure 14. Long term distribution of wind speeds – curve fitting – direction 45°

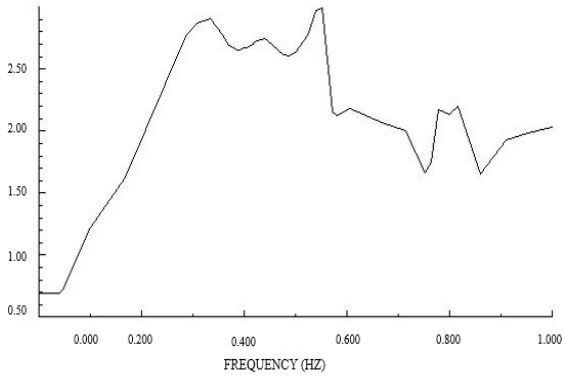


Figure 15. Hot-spot stress spectrum (wave induced)

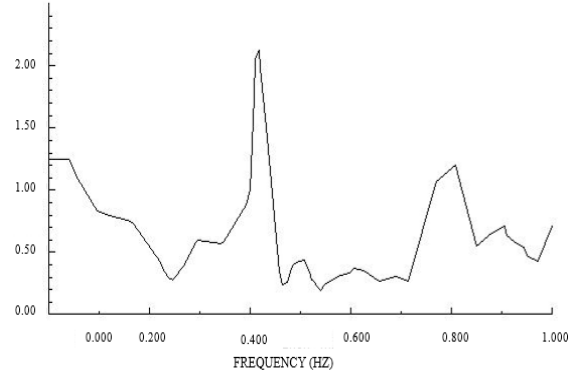


Figure 16. Hot-spot stress spectrum (wind induced)

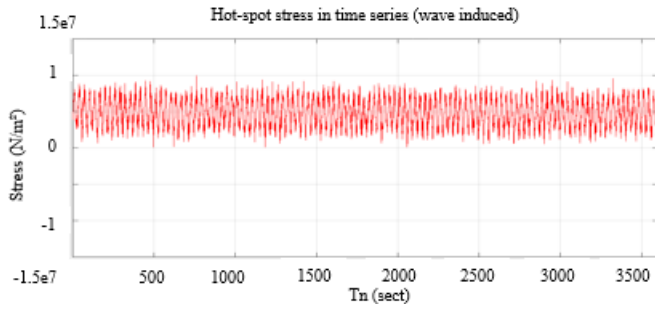


Figure 17. Hot-spot stress in time series (wave induced)

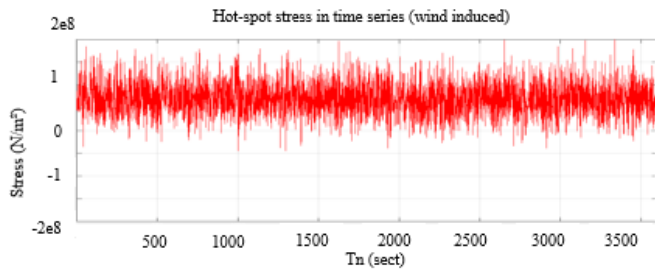


Figure 18. Hot-spot stress in time series (wind induced)

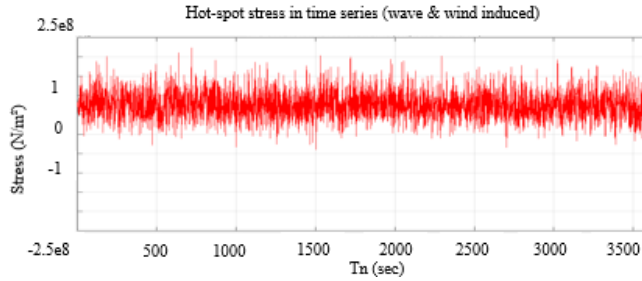


Figure 19. Hot-spot stress in time series (wave and wind induced)

Fatigue damage at high-concentrated stress points (hot-spots) is calculated by evaluating the hot-spot stress range (HSSR) and make use of this as input data for S-N fatigue curve. The stress concentration factors (SCF) is defined as following:

$$SCF = HSSR / \text{Nominal Stress Range} \quad (24)$$

For all concentric masses of the structure system, the SCF coefficient will be taken as 2.0 in this paper.

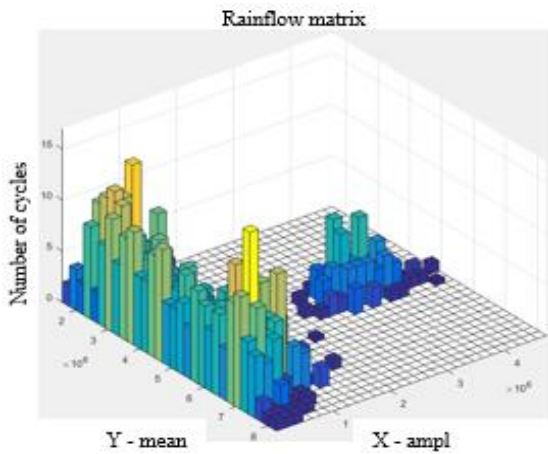


Figure 20. Rain-flow matrix at hot-spot point due to wave

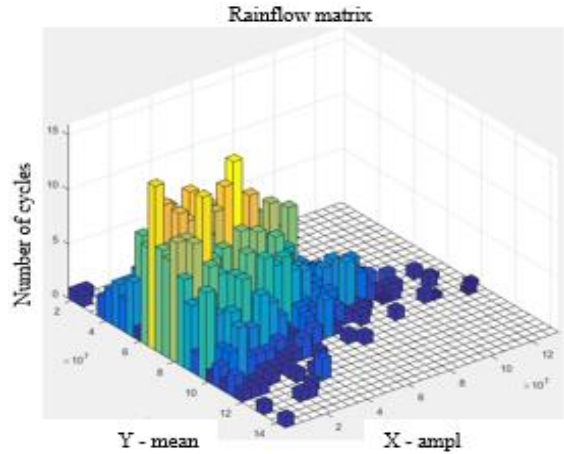


Figure 21. Rain-flow matrix at hot-spot point due to wind

Corresponding to each hot-spot stress in time series, the rain-flow method is applied here under aiding of MATLAB software so that the rain-flow matrices at different hot-spot points due to wave and wind are obtained without any trouble as shown in Figs. 20 and 21. Finally, the rain-flow matrices due to wave and wind interaction can be easily obtained in the same manner and the result can be seen in Fig. 22.

Some cycles that are counted with the amplitude and average stress value at the hot-spot point can be extracted from the rain-flow matrix. This type of matrix has been widely applied for fatigue analysis because of its simple form, time-saved computing, and its expression provides general information on the nature of loads [15]. As mentioned earlier, Palmgren-Miner's hypothesis assumes that the total of fatigue damage is calculated by taking a linear combination of any individual cycles. The fatigue life of structure at each hot-spot is listed in Tables 5, 6 and 7 (the mean wind velocity: 17.5 m/s)

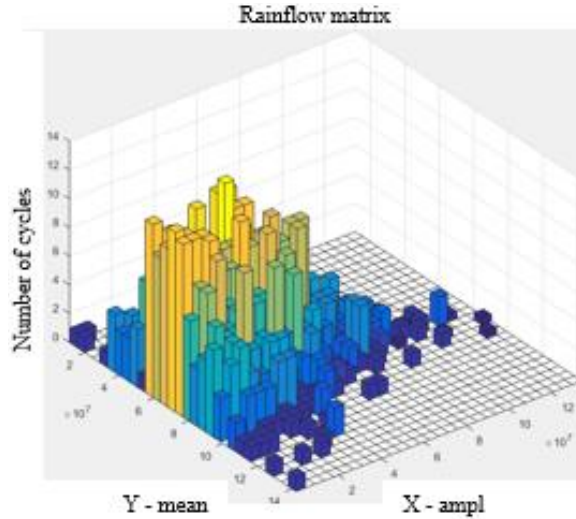


Figure 22. Rain-flow matrix at hot-spot point due to both wave and wind

Table 5. Fatigue life of OWT support structure (wave induced)

No.	[D]	T (sec)	Node type	Chord (cm)		Fatigue life (year)	Status
				OD	WT		
1	0.5	3600	Y	70	2	829.25	Ok
2	0.5	3600	Y	70	2	561.36	Ok
3	0.5	3600	Y	70	2	996.15	Ok
4	0.5	3600	X	80	2	937.57	Ok
5	0.5	3600	X	120	4.5	1005.21	Ok
6	0.5	3600	X	120	4.5	1258.02	Ok

Table 6. Fatigue life of OWT support structure (wind induced)

No.	[D]	T (sec)	Node type	Chord (cm)		Fatigue life (year)	Status
				OD	WT		
1	0.5	3600	Y	70	2	197.81	Ok
2	0.5	3600	Y	70	2	151.26	Ok
3	0.5	3600	Y	70	2	196.21	Ok
4	0.5	3600	X	80	2	271.26	Ok
5	0.5	3600	X	120	4.5	306.12	Ok
6	0.5	3600	X	120	4.5	465.32	Ok
7	0.5	3600	Y	70	2	182.13	Ok

Apart from the result of mean wind velocity 17.5 m/s, Fig. 23 shows the fatigue life curve of OWT due to different velocities, whereas there are mean wind velocities that are greater than the cut-out mean wind velocity.

Table 7. Fatigue life of OWT support structure (wave and wind induced)

No.	[D]	T (sec)	Node type	Chord (cm)		Fatigue life (year)	Status
				OD	WT		
1	0.5	3600	Y	70	2	176.38	Ok
2	0.5	3600	Y	70	2	132.58	Ok
3	0.5	3600	Y	80	2	273.32	Ok
4	0.5	3600	X	80	2	278.51	Ok
5	0.5	3600	X	120	4.5	291.46	Ok
6	0.5	3600	X	120	4.5	452.96	Ok
7	0.5	3600	Y	70	2	172.34	Ok

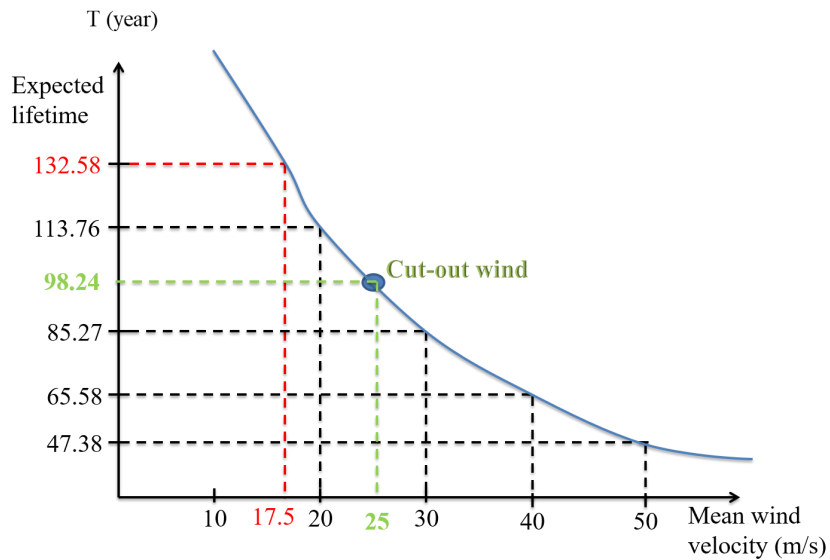


Figure 23. The fatigue life curve of OWT corresponding to each mean wind velocity

6. Conclusions

To calculate the fatigue life of OJWT, in the scope of the paper, a wind turbine model with jacket support structure in the water depth of 70 m is utilized. All blades, turbine machine and machine-support tower are simplified into support tower that mass is concentrated on top and is supported by jacket structure. In terms of wind data, Weibull distribution is used to generate input data for fatigue analysis of OJWT. Wind and wind-induced wave loads act on structure in stochastic directions, however, only 08 directions are considered with evenly spaced 45-degree angle to compute fatigue life of each components' jacket support structure. The Airy wave theory is applied for computing the static and dynamic transfer function of wave to support the fatigue analysis, and further study should be utilized different wave theories. The results are rather reasonable since the simultaneous interaction between wind and wind-induced wave is considered.

References

- [1] Zachary, S. (2014). *History of wind turbines*. Renewable Energy World.
- [2] Tempel, J. (2002). *Offshore wind, to mill or to be milled*. Delf University of Technology.
- [3] BTM Consult ApS (2005). *International wind energy development, world market update 2004, Forecast 2005-2009*. IC Christensens Allé 1, DK6950 Ringkøbing, Denmark.
- [4] Jingpeng, H., Zitang, S., Yanxia, L. (2012). *Simulation of turbulent wind velocity for transmission tower based on auto-Regressive model method*. School of Civil Engineering, Northeast Dianli University, Jilin, China.
- [5] Petrini, F., Li, H., Bontempi, F. (2010). [Basis of design and numerical modeling of offshore wind turbines](#). *Structural Engineering & Mechanics*, 36(5):599–624.
- [6] U.S. Army Corps of Engineers (2006). *Coastal engineering manual*. Part II, EM 1110-2-1100.
- [7] Mathisen, J., Bitner-Gregersen, E. (1990). [Joint distributions for significant wave height and wave zero-up-crossing period](#). *Applied Ocean Research*, 12(2):93–103.
- [8] Thoft-Cristensen, P., Baker, M. J. (1982). *Structural reliability theory and its applications*. Springer-Verlag, Berlin Heidelberg, New York.
- [9] Pierson Jr, W. J., Moskowitz, L. (1964). A proposed spectral form for fully developed wind seas based on the similarity theory of SA Kitaigorodskii. *Journal of Geophysical Research*, 69(24):5181–5190.
- [10] Hasselmann, K., Barnett, T. P., Bouws, E., Carlson, H., Cartwright, D. E., Enke, K., Ewing, J. A., Gienapp, H., Hasselmann, D. E., Kruseman, P., Meerburg, A., Muller, P., Olbers, D. J., Richter, K., Sell, W., Walden, H. (1973). *Measurements of wind-wave growth and swell decay during the Joint North Sea Wave Project (JONSWAP)*. Deutsches Hydrographisches Zeitschrift, Hamburg, Reihe A.
- [11] Bartrop, N. D. P., Adams, A. J. (1991). *Dynamics of fixed marine structures*. Atkins Oil & Gas Engineering Limited, Epsom, UK.
- [12] Li, Y. Q., Dong, S. L. (2001). Random wind load simulation and computer program for large-span spatial structures. *Spatial Structures*, 7(3):3–11.
- [13] Matsuiski, M., Endo, T. (1969). *Fatigue of metals subjected to varying stress*. Japan Soc. Mech. Eng.
- [14] Vandijk, G. M., Dejonge, J. B. (1975). *Introduction to a fighter aircraft loading standard for fatigue evaluation*. FALSTAFF, National Aerospace Laboratory, NLR, MP75017U, Amsterdam, Holland.
- [15] Adam, N. (2009). *Determination of fragments of multi-axial service loading strongly influencing the fatigue of machine components*. Mechanical Systems and Signal Processing.